PHYSICAL REVIEW B **67**, 060501(R) (2003)

Systematics of electronic structure and interactions in $Bi_2Sr_2Ca_{n-1}Cu_nO_{2n+4}$ $(n=1-3)$ by angle-resolved photoemission spectroscopy

H. Matsui,[1] T. Sato,[1] T. Takahashi,[1] H. Ding,[2] H.-B. Yang,[2] S.-C. Wang,[2] T. Fujii,[3,*] T. Watanabe,[4,†] A. Matsuda,[3,4] T. Terashima,[5] and K. Kadowaki[6]

[1]*Department of Physics, Tohoku University, Sendai 980-8578, Japan*
[2]*Department of Physics, Boston College, Chestnut Hill, Massachusetts 02467*
[3]*Department of Applied Physics, Faculty of Science, Science University of Tokyo, Tokyo 162-8601, Japan*
[4]*NTT Basic Research Laboratories, Atsugi 243-0198, Japan*
[5]*Institute for Chemical Research, Kyoto University, Uji 611-0011, Japan*
[6]*Institute of Materials Science, University of Tsukuba, Ibaraki 305-3573, Japan*

(Received 19 November 2002; published 28 February 2003)

We have performed systematic angle-resolved photoemission spectroscopy on the high-T_c superconducting family of $Bi_2Sr_2Ca_{n-1}Cu_nO_{2n+4}$ $(n=1-3)$. In addition to the generic features of the large Fermi surface and *d*-wave superconducting gap, we have found that there exists a scaling of the doping dependence of the energy gap. Moreover, comparison of the nodal dispersion in the superconducting state shows that the ''kink'' (the sudden change of band dispersion), while occurring at a similar binding energy, becomes more pronounced with increasing layer number *n*, indicating stronger coupling between electrons and a collective mode.

DOI: 10.1103/PhysRevB.67.060501 PACS number(s): 74.72.Hs, 71.18.+y, 74.25.Jb, 79.60.Bm

It has been well established that the CuO_2 plane is a key block in the crystal structure to realize the high-temperature (high-T_c) superconductivity in cuprates. It is empirically known that the superconducting-transition temperature (T_c) increases with an increasing number of CuO_2 planes (n) in a unit cell of the crystal. For example, in Bi-family high-T_c superconductors (HTSCs), T_c increases from 10 K for single-layered $Bi_2Sr_2CuO_6$ (Bi2201) to 90 K for bilayered $Bi_2Sr_2CaCu_2O_8$ (Bi2212), and further to 110 K for trilayered $Bi_2Sr_2Ca_2Cu_3O_{10}$ (Bi2223). This suggests that the interlayer interaction is important to achieve higher T_c and that there may be a certain universal rule relating to *n*. However, despite intensive theoretical and experimental studies, the microscopic origin to enhance T_c in multilayered cuprates is still unknown. It is thus urgently required to clarify differences and similarities in the electronic structure, in particular in the low-energy excitation which directly relates to the superconductivity, among single- to multilayered high-T_c cuprates. Angle-resolved photoemission spectroscopy (ARPES) has revealed the essential electronic structure of high-T_c cuprates such as Fermi surface[1,2] and superconducting gap.[3,4] Recent improvement in the energy resolution in ARPES has enabled direct observation of low-energy excitation[5–7] as well as the interaction between two CuO_2 planes (bilayer band splitting).[8,9] However, in contrast to intensive ARPES studies on bilayered cuprates (Bi2212), few ARPES works to systematically study the electronic structure near the Fermi level (E_F) as a function of CuO_2 planes have been reported. This is because of the difficulty in growing a high-quality trilayered single crystal (Bi2223). Comparison among these three Bi-family HTSCs would reveal not only the basic electronic structure irrespective of the number of CuO_2 planes (n), but also, more importantly, the difference in the low-energy excitation for different *n* compounds, which is crucial to find key parameter(s) to enhance T_c in multilayered high-T_c cuprates.

In this paper, we report systematic high-resolution ARPES on $Bi_2Sr_2Ca_{n-1}Cu_nO_{2n+4}$ $(n=1-3)$ single crystals. By comparing the experimental result for $n=3$ with those for $n=1$ and 2, we discuss the universality and speciality of the basic electronic structure near E_F in these three high-T_c cuprates, such as the Fermi-surface (FS) topology, the superconducting-gap symmetry, and the doping dependence of the superconducting gap. We also discuss the coupling strength of electrons with collective mode(s) as a function of *n* to study the microscopic origin to enhance T_c in multilayered cuprates.

High-quality $Bi_2Sr_2Ca_{n-1}Cu_nO_{2n+4}$ $(n=1-3)$ single crystals were grown by the traveling solvent floating-zone (TSFZ) method. Details of sample preparations have been described elsewhere.[10,11] ARPES measurements were performed with a GAMMADATA-SCIENTA SES-200 spectrometer at the undulator 4m-NIM beamline of the Synchrotron Radiation Center, University of Wisconsin-Madison, Wisconsin, as well as with a same-type spectrometer using a high-flux discharge lamp and a toroidal grating monochromator at Tohoku University, Japan. We used 22-eV synchrotron photons and a He $I\alpha$ resonance line (21.218 eV) to excite photoelectrons. The energy and angular (momentum) resolutions were set at 9–15 meV and 0.2° (0.007 $Å^{-1}$), respectively. Samples were cleaved *in situ* in an ultrahigh vacuum of $4-8\times10^{-11}$ Torr to obtain a clean surface for measurement. The Fermi level (E_F) of samples was referred to that of a gold film deposited on a metallic substrate which is in electrical contact with samples.

Figure 1 shows ARPES-intensity maps of Bi2223 as a function of the two-dimensional wave vector for an underdoped sample with $T_c=100$ K (UD100K) and an overdoped one with $T_c=108$ K (OD108K). ARPES intensity is integrated over the energy range of 50 meV centered at E_F. Measurements were done in the *Y* quadrant to avoid the complication from the superlattice bands.[2] Two intensity maxima symmetric to the *M* point are clearly seen on M-$Y(X)$ line,

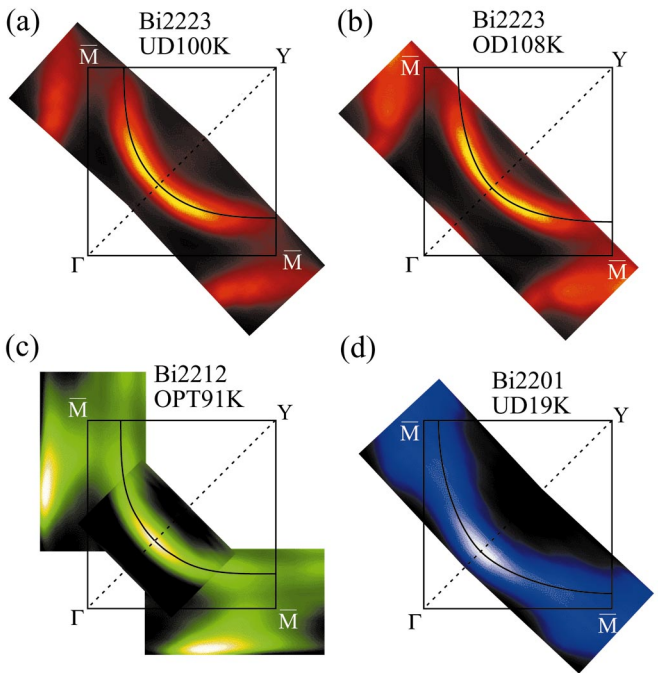

FIG. 1. (Color) Plots of ARPES intensity integrated within ±50 meV centered at E_F for (a) Bi2223 UD100K, (b) Bi2223 OD108K, (c) Bi2212 OPT91K, and (d) Bi2201 (Pb-substituted) UD19K.

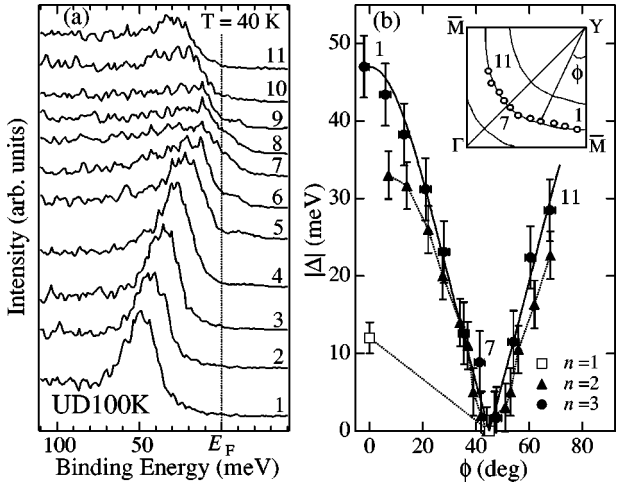

FIG. 2. (a) ARPES spectra of Bi2223 (UD100K) in the superconducting state ($T=40$ K) measured at various k_F points shown in inset of (b). (b) Momentum dependence of the superconducting gap (Δ) for $n=1$–3 as a function of FS angle (ϕ) (Refs. 4 and 16). Solid line for Bi2223 represents the best fit using the gap function: $\Delta(k)=\Delta_{max}\,[\mathrm{Bcos}(2\phi)+(1-B)\cos(6\phi)]$ (Ref. 17).

but not on the Γ-M line. This clearly defines a large holelike FS centered at $X(Y)$ for both samples, consistent with a recent report.[12] We have determined the Fermi vector (k_F) by fitting the momentum distribution curves (MDCs) and estimated the FS volume to be 56±2% and 59±2% of the whole Brillouin zone for UD100K and OD108K samples, respectively. These values correspond to $x=0.12\pm0.03$ and 0.17 ± 0.03 where $1+x$ is the hole count, consistent with the doping level, since the doping level at the optimally doped region is typically $x=0.16$.[13] In Figs. 1(c) and (d), we plot the ARPES intensity for Bi2212 (OPT91K: optimally doped, $T_c=91$ K) and Bi2201 (UD19K: underdoped, $T_c=19$ K). One can clearly see that ARPES-intensity distributions are essentially similar to that in Bi2223, showing that the holelike Fermi surface is a generic feature of the CuO_2 plane in HTSCs. It is also noted that the trilayer splitting is not clearly resolved in Bi2223, since the MDC can be fitted by a single Lorentzian. This may be due to the difference in the spectral weight distribution between Bi2223 and bilayer Bi2212, as suggested by recent theoretical[14] and ARPES studies.[12]

Figure 2(a) shows ARPES spectra near E_F for the UD100K Bi2223 sample in the superconducting state (40 K) measured on the Fermi surface (k_F points) in the Y quadrant [see the inset to Fig. 2(b)]. A sharp quasiparticle (QP) peak is located about 50-meV away from E_F near the M point (spectrum 1), and gradually moves towards E_F when approaching the nodal line. No sizable leading-edge shift is observed in spectra 7–9. This momentum dependence of QP peaks clearly indicates the highly anisotropic nature of the superconducting gap in underdoped Bi2223, similar to the optimally doped Bi2223.[12] In order to estimate the superconducting-gap size (Δ) more accurately, we have symmetrized the spectra with respect to E_F (Ref. 15) and fit each curve by two Lorentzians symmetric to E_F. The obtained k dependence of Δ is shown in Fig. 2(b), together with those of Bi2201 and Bi2212.[4,16] The overall "V" shape of the gap curve, as well as the node along the Γ-Y line ($\phi=45°$), strongly support the d-wave nature of the gap in all Bi-family HTSCs. We have fit the gap size for Bi2223 as a function of ϕ by using the formula $\Delta(\phi)=\Delta_{max}[\mathrm{Bcos}(2\phi)+(1\text{-B})\cos(6\phi)]$, where the $\cos(6\phi)$ term represents the second harmonic of the $d_{x^2-y^2}$-gap function.[17] Excellent agreement is obtained with the parameters $\Delta_{max}=47$ meV and $B=0.94$. A small but finite amount of the second term (6%) may be due to the underdoped nature of the sample.[17] It is noted here when we compare the gap size among $n=1$–3, we find that the overall gap value systematically increases with increasing n, demonstrating a certain scaling of the superconducting gap.[18]

Next we study the doping dependence of Δ_{max}. Figure 3(a) shows ARPES spectra at the superconducting state (40 K), measured at k_F on the M-Y line ($\phi=0°$) for three Bi2223 samples with different dopings (UD100K, OPT108K, and OD108K). Although the overall spectral feature such as the hump-dip-peak structure looks similar, there are quantitative differences in the spectra. When the doping is increased from UD100K to OD108K, the intensity of the QP peak is gradually enhanced and at the same time the peak position (Δ_{max}) systematically moves toward E_F, consistent with similar behavior observed in Bi2212.[5] The increase in the QP-peak intensity is consistent with the increase in the superfluid density as the hole doping is increased.[19,20] In order to estimate Δ_{max} quantitatively, we have fit the ARPES spectra by a Gaussian for the QP peak and a linear function

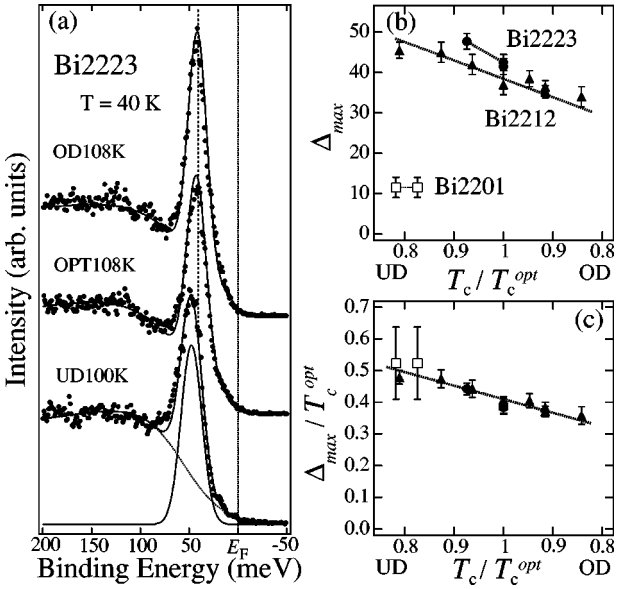

FIG. 3. (a) Doping dependence of ARPES spectra of Bi2223 in the superconducting state (40 K) measured at M-Y crossing for three doping levels (UD100K, OPT108K, OD108K). Solid lines represent the numerical fittings. The dashed straight line around 40 meV is a guide for the eyes. (b) Comparison of the doping dependence of Δ_{max} among Bi-family HTSCs (Refs. 16 and 20). (c) Same as for (b) but normalized with T_c^{opt}.

with an asymmetric cutoff for the hump.[19,20] Both are multiplied by the Fermi-Dirac function and then convoluted by a Gaussian with a width of the instrumental resolution. Figure 3(b) plots obtained Δ_{max} as a function of T_c/T_c^{opt} where T_c^{opt} is the T_c at optimal doping, compared with those of Bi2201 (Ref. 16) and Bi2212 obtained by the same fitting procedure.[20] Both Bi2223 and Bi2212 show a general trend in which Δ_{max} decreases with increasing doping. It is also evident that Δ_{max} of Bi2223 is larger than that of Bi2212 at a fixed doping level. The Δ_{max} of Bi2212 is on average 0.85 of that of Bi2223, which is close to the ratio of T_c (91 K/108 K=0.84). This suggests a similar $2\Delta_{max}/k_BT_c$ value for both compounds, consistent with a recent break junction tunneling experiment on Bi2223.[21] In fact, as shown in Fig. 3(c), when we normalize Δ_{max} with T_c^{opt} for each compound, we find that all these compounds show a very similar Δ_{max}/k_BT_c value at a fixed doping level. This suggests a scaling in the doping dependence of the energy gap among the three compounds.

Finally, we examine band dispersion along the nodal direction. Figure 4 shows the energy dispersions near E_F in the superconducting state measured along Γ-Y for nearly optimally doped Bi2201, Bi2212, and Bi2223. We find that although the normal-state dispersion is almost identical for three compounds, they have a noticeable difference in the superconducting state as explained below. It is established that the nodal dispersion shows a characteristic bending behavior (''kink'') near E_F, which is attributed to the coupling between electrons and a certain mode. We find in Fig. 4(c) that a ''kink'' is also present in Bi2223 and it has almost the same binding energy (50–80 meV) as in Bi2201 and Bi2212.

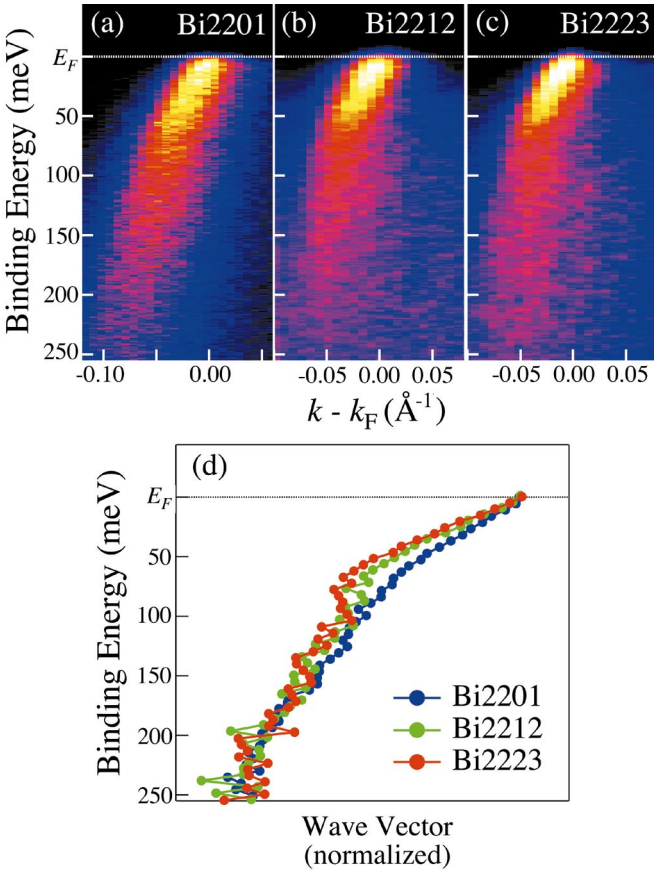

FIG. 4. (Color) ARPES-intensity plots along the Γ-Y direction in the superconducting state for nearly optimally doped Bi-family HTSCs, (a) Bi2201 (Pb-substituted; T_c=19 K), (b) Bi2212 (T_c=91 K), and (c) Bi2223 (T_c=108 K). (d) MDC peak dispersions for three samples after normalizing the wave vector. The normalization of the wave vector is performed by aligning three dispersions so as to pass the same point at E_F and 250 meV. The MDC peak position at 250 meV is obtained by smoothing each MDC.

Remarkably, when we normalize the wave vector so as to align the peak at E_F and the highest binding energy (250 meV), the dispersions near E_F show a systematic difference among three compounds as shown in Fig. 4(d). It is evident that the ''kink'' in dispersion becomes more pronounced as n increases. This observation strongly suggests that the coupling strength increases with the number of CuO_2 layers in a unit cell and consequently the maximum T_c. A similar behavior, indicative of the stronger coupling with larger n, is also observed in the ARPES spectral line shape around the M point, where the ''peak-dip-hump'' structure becomes more pronounced with larger n.[18] This similarity in the n dependence suggests the same origin for the ''kink'' structure along the nodal direction and the ''peak-dip-hump'' around the M point in the superconducting state.

The results in Figs. 4 and 3(b) imply an important nature of the many-body effect in the low-energy excitations. We found that the coupling constant and the Δ_{max} increase with increasing n (maximum T_c), pointing to a possible correlation between these two important physical parameters. Furthermore, the present ARPES result also puts a constraint on

interpreting a microscopic origin of the coupling between electrons and the collective mode. If the coupling is purely due to the longitudinal-optical phonon,[6] the present ARPES result suggests that the phonon density of states (or dispersion) should show a systematic difference with n, whereas the representative phonon frequencies look similar to each other (50–80 meV). On the other hand, if the coupling is from the magnetic mode,[5,7,22,23] it is expected that the intensity of the resonance peak around $Q=(\pi,\pi)$ in inelastic neutron-scattering (INS) experiments increases with increasing n. Recently Kee *et al.*[24] reported that the intensity of the magnetic-resonance peak is too small to account for the significant kink features observed by ARPES. If this is the case, it raises another question as to why the temperature dependence of the strength of the kink closely resembles that of the resonance-peak intensity.[7,22] Further comprehensive comparison between ARPES and INS could clarify these important issues in the low-energy electron dynamics of HTSCs.

In conclusion, we have performed systematic high-resolution angle-resolved photoemission spectroscopy of Bi-family HTSCs. We have shown that the holelike Fermi surface and the $d_{x^2-y^2}$-like superconducting gap are generic features of the CuO_2 plane, irrespective of the number of layers in a unit cell. In addition, we have found a scaling rule in the doping dependence of the energy gap for three compounds. Comparison of the nodal dispersion in the superconducting state has also revealed that the interaction of electrons with mode is stronger for larger n.

We thank M. Mori, T. Tohyama, J. R. Engelbrecht, and Z. Wang for useful discussions. This work was supported by a Grant-in-Aid for Scientific Research from MEXT of Japan, the U.S. National Science Foundation (NSF) Grant No. DMR-0072205, and the Sloan Foundation. T.S. thanks the Japan Society for Promotion of Science for financial support. The Synchrotron Radiation Center is supported by U.S. NSF Grant No. DMR-0084402.

*Present address: Department of Applied Physics, Waseda University, Tokyo 169-8555, Japan.

†Present address: NTT Photonics Laboratories, Atsugi 243-0198, Japan.

[1] P. Aebi *et al.*, Phys. Rev. Lett. **72**, 2757 (1994).
[2] H. Ding *et al.*, Phys. Rev. Lett. **76**, 1533 (1996).
[3] Z.-X. Shen *et al.*, Phys. Rev. Lett. **70**, 1553 (1993).
[4] H. Ding *et al.*, Phys. Rev. B **54**, R9678 (1996).
[5] J.C. Campuzano *et al.*, Phys. Rev. Lett. **83**, 3709 (1999).
[6] A. Lanzara *et al.*, Nature (London) **412**, 510 (2001).
[7] P.D. Johnson *et al.*, Phys. Rev. Lett. **87**, 177007 (2001).
[8] D.L. Feng *et al.*, Phys. Rev. Lett. **86**, 5550 (2001).
[9] Y.-D. Chuang *et al.*, Phys. Rev. Lett. **87**, 117002 (2001).
[10] T. Fujii, T. Watanabe, and A. Matsuda, J. Cryst. Growth **223**, 175 (2001).
[11] I. Chong *et al.*, Physica B **290C**, 57 (1997).
[12] D.L. Feng *et al.*, Phys. Rev. Lett. **88**, 107001 (2002).
[13] M.R. Presland *et al.*, Physica C **176**, 95 (1991).
[14] M. Mori, T. Tohyama, and S. Maekawa, Phys. Rev. B **66**, 064502 (2002).
[15] M.R. Norman *et al.*, Nature (London) **392**, 157 (1998).
[16] T. Sato *et al.*, Phys. Rev. B **63**, 132502 (2001).
[17] J. Mesot *et al.*, Phys. Rev. Lett. **83**, 840 (1999).
[18] T. Sato *et al.*, Phys. Rev. Lett. **89**, 067005 (2002).
[19] D.L. Feng *et al.*, Science **289**, 277 (2000).
[20] H. Ding *et al.*, Phys. Rev. Lett. **87**, 227001 (2001).
[21] T. Ekino *et al.*, Phys. Rev. B **64**, 092510 (2001).
[22] A.D. Gromko *et al.*, cond-mat/0202329 (unpublished).
[23] S.V. Borisenko *et al.*, cond-mat/0209435 (unpublished).
[24] H.-Y. Kee, S.A. Kivelson, and G. Aeppli, Phys. Rev. Lett. **88**, 257002 (2002).